Regular Article

blood

MYELOID NEOPLASIA

DOT1L as a therapeutic target for the treatment of *DNMT3A*-mutant acute myeloid leukemia

Rachel E. Rau,[1,2] Benjamin A. Rodriguez,[2,3] Min Luo,[4-6] Mira Jeong,[4-6] Allison Rosen,[4-6] Jason H. Rogers,[1] Carly T. Campbell,[7] Scott R. Daigle,[7] Lishing Deng,[8] Yongcheng Song,[8] Steve Sweet,[9] Timothy Chevassut,[10] Michael Andreeff,[11] Steven M. Kornblau,[11] Wei Li,[2,3] and Margaret A. Goodell[1,2,4-6]

[1]Department of Pediatrics, Baylor College of Medicine and Texas Children's Hospital, Houston, TX; [2]Dan L. Duncan Cancer Center, [3]Department of Molecular and Cellular Biology, [4]Department of Molecular and Human Genetics, [5]Stem Cells and Regenerative Medicine Center, and [6]Center for Cell and Gene Therapy, Baylor College of Medicine, Houston, TX; [7]Epizyme, Inc., Cambridge, MA; [8]Department of Pharmacology, Baylor College of Medicine, Houston, TX; [9]Genome Damage and Stability Centre, and [10]Department of Haematology, Brighton and Sussex Medical School, University of Sussex, Brighton, United Kingdom; and [11]Department of Leukemia, The University of Texas MD Anderson Cancer Center, Houston, TX

Key Points

- Data from *Dnmt3a*$^{-/-}$ mice implicate Dot1l as a critical mediator of the malignant gene expression program of *Dnmt3a*-mediated leukemia.
- Pharmacologic inhibition of DOT1L exerts potent antileukemic activity in *DNMT3A*-mutant human acute myeloid leukemia in vitro and in vivo.

Mutations in DNA methyltransferase 3A (*DNMT3A*) are common in acute myeloid leukemia and portend a poor prognosis; thus, new therapeutic strategies are needed. The likely mechanism by which *DNMT3A* loss contributes to leukemogenesis is altered DNA methylation and the attendant gene expression changes; however, our current understanding is incomplete. We observed that murine hematopoietic stem cells (HSCs) in which *Dnmt3a* had been conditionally deleted markedly overexpress the histone 3 lysine 79 (H3K79) methyltransferase, Dot1l. We demonstrate that *Dnmt3a*$^{-/-}$ HSCs have increased H3K79 methylation relative to wild-type (WT) HSCs, with the greatest increases noted at DNA methylation canyons, which are regions highly enriched for genes dysregulated in leukemia and prone to DNA methylation loss with *Dnmt3a* deletion. These findings led us to explore DOT1L as a therapeutic target for the treatment of *DNMT3A*-mutant AML. We show that pharmacologic inhibition of DOT1L resulted in decreased expression of oncogenic canyon–associated genes and led to dose- and time-dependent inhibition of proliferation, induction of apoptosis, cell-cycle arrest, and terminal differentiation in *DNMT3A*-mutant cell lines in vitro. We show in vivo efficacy of the DOT1L inhibitor EPZ5676 in a nude rat xenograft model of *DNMT3A*-mutant AML. DOT1L inhibition was also effective against primary patient *DNMT3A*-mutant AML samples, reducing colony-forming capacity (CFC) and inducing terminal differentiation in vitro. These studies suggest that DOT1L may play a critical role in *DNMT3A*-mutant leukemia. With pharmacologic inhibitors of DOT1L already in clinical trials, DOT1L could be an immediately actionable therapeutic target for the treatment of this poor prognosis disease. (*Blood*. 2016;128(7):971-981)

Introduction

Mutations of the de novo DNA methyltransferase DNA methyltransferase 3A (*DNMT3A*) occur in approximately 20% of all adult patients with acute myeloid leukemia (AML). Studies indicate that patients with *DNMT3A* mutations suffer particularly poor prognoses, indicating novel therapies are needed.[1-4] *DNMT3A* mutations in AML are almost exclusively heterozygous, and approximately 60% affect the arginine at amino acid position 882 (R882) in the methyltransferase domain. R882-mutant DNMT3A is a hypomorphic protein that also inhibits the remaining WT DNMT3A, dramatically reducing cellular DNA methyltransferase activity[5,6]; however, the exact mechanisms by which DNMT3A loss contributes to leukemogenesis are poorly understood. DNA methylation profiling of *DNMT3A*-mutant AML samples revealed loci with decreased methylation, but, surprisingly, also a small subset of loci with increased methylation.[1,4,7,8] These data suggest the pathologic changes in DNA methylation are mediated by additional, unknown factors.

Conditional ablation of *Dnmt3a* in the murine hematopoietic system results in a dramatic expansion of hematopoietic stem cells (HSCs), a progressive block in differentiation,[9] and priming for malignant transformation.[10,11] Whole genome bisulfite sequencing of *Dnmt3a*$^{-/-}$ HSCs revealed that the borders of expansive undermethylated regions, termed methylation canyons, are hotspots for DNA methylation loss, which leads to expansion of the canyon.[12] Canyons that expand with *Dnmt3a* deletion are highly enriched for genes dysregulated in human leukemia, including *HOX* genes,[12] suggesting these sites are important in leukemogenesis. Analysis of The Cancer Genome Atlas data confirmed many of these sites have methylation loss in *DNMT3A*-mutant AML[8,12]; and many canyon-associated genes,

Submitted November 24, 2015; accepted June 6, 2016. Prepublished online as *Blood* First Edition paper, June 22, 2016; DOI 10.1182/blood-2015-11-684225.

The online version of this article contains a data supplement.

The publication costs of this article were defrayed in part by page charge payment. Therefore, and solely to indicate this fact, this article is hereby marked "advertisement" in accordance with 18 USC section 1734.

including *HOX* genes, are significantly changed in *DNMT3A*-mutant AML.[4,8,12]

In addition to the DNA methylation changes in *Dnmt3a*$^{-/-}$ HSCs, chromatin immunoprecipitation (ChIP)-sequencing (seq) and RNA-seq data revealed evidence of perturbations of histone modifications. Given the known functional interaction between DNA methylation and histone modifications, these alterations were intriguing.[13-16] The observed overexpression of the histone 3, lysine 79 (H3K79) methyltransferase, Dot1l (disrupter of telomere silencing 1-like), was especially interesting because it plays a critical role in leukemia with *MLL* rearrangements.[17-20] Pharmacologic inhibition of DOT1L has shown promising preclinical activity in *MLL*-rearranged leukemia and is now being tested in adult and pediatric clinical trials.[21-25] *MLL* rearrangements rarely cooccur with *DNMT3A* mutations in AML.[3,4,7] The essential mutual exclusivity[7] of these lesions and the overexpression of Dot1l in our murine model led us to hypothesize that *MLL* rearrangements and *DNMT3A* mutations are distinct epigenetic aberrations that converge on a common mechanism, resulting in dysregulated gene expression mediated by H3K79 methylation. We therefore explored the role of DOT1L in *DNMT3A*-mediated leukemia and evaluated DOT1L as a therapeutic target for the treatment of this disease with a poor prognosis.

Methods

Murine model

Animal procedures were approved by the Animal Care and Use Committee of Baylor College of Medicine. For ChIP-seq experiments, C57Bl/6 CD45.2 *Dnmt3a*$^{fl/fl}$ and *Dnmt3a*$^{WT/WT}$ were crossed to Rosa26-Cre ER^{T2}.[26] *Dnmt3a*$^{fl/fl}$-Rosa26-Cre ER^{T2} and *Dnmt3a*$^{WT/WT}$-Rosa26-Cre ER^{T2} mice were treated with 5 daily intraperitoneal injections of tamoxifen (1 mg/0.1 mL corn oil per mouse per day) to induce deletion of the floxed Dnmt3a allele. This typically results in a >80% biallelic deletion as determined by genotyping of individual MethoCult colonies from the bone marrow of *Dnmt3a*$^{fl/fl}$-Rosa26-Cre ER^{T2} after tamoxifen treatment. Eight weeks later, bone marrow was harvested and transplanted (1×10^6 per mouse) into lethally irradiated syngeneic CD45.1 recipients. Additional details of murine experiments are provided in the supplemental Methods, available on the *Blood* Web site.

ChIP-seq

Four months after transplantation, recipient mice were euthanized, and pooled bone marrow HSCs from *Dnmt3a*$^{-/-}$ and control mice were purified using c-Kit magnetic enrichment (AutoMACS; Miltenyi Biotec) followed by gating on live cells and sorting for lineage$^-$, Sca1$^+$, CD48$^-$, and CD150$^+$ cells (FACSAria; BD Biosciences; antibodies from Becton Dickinson). ChIP-seq was performed on purified HSCs after chromatin crosslinking with 1% formalin followed by cell lysis in sodium dodecyl sulfate buffer. DNA was fragmented by sonication and ChIP performed using anti-H3K79me2 (ab3594; Abcam). Eluted DNA was used to prepare a library (Illumina ChIP-seq kit) and then sequenced on an Illumina HiSequation (100-base paired-end). Raw reads were quality trimmed (Trimgalore) and mapped (mm9) (Bowtie 2.0.6). See the supplemental Methods for details of analyses performed. Reviewers may access a track hub for H3K79me2 in the mouse genome (mm9) at: http://genome.ucsc.edu/cgi-bin/hgTracks?db5mm9&hubUrl5http://dldcc-web.brc.bcm.edu/lilab/benji/RaRau/k79.hub.txt.

Cell culture and reagents

Human leukemia cell lines OCI AML3 and OCI AML2 were provided by Mark Minden (Ontario Cancer Institute). Cells were grown in RPMI-1640 (Invitrogen) plus 10% fetal bovine serum, 1% L-glutamine, and 1% pen strep at 37°C in 5% carbon dioxide. Cell lines were validated by the short tandem repeat method. For in vitro experiments, we used DOT1L inhibitors SYC-522[21] and EPZ004777[23] (Epizyme, Inc). For in vivo studies, EPZ-5676[22] (Epizyme, Inc.) was used.

Cell proliferation, viability, and colony formation assays

Exponentially growing cells were plated in triplicate in 24-well plates (2×10^5/mL; final volume 1 mL). For dose-dependent assays, cells were incubated in increasing concentrations of SYC522[21] or EPZ004777[23] or dimethyl sulfoxide (DMSO) control. For time-dependent assays, cells were incubated in 3 μM EPZ004777[23] or DMSO control. Every 2 to 3 days, media and compound were replaced and cells were split to 2×10^5/mL. At each replating, the viable cell number was determined (trypan blue). Total cell number is expressed as split-adjusted viable cells per milliliter. Analysis of apoptosis, cell-cycle, and cellular differentiation and gene expression changes were performed as described in the supplemental Methods. Viably frozen primary AML samples (obtained from MD Anderson Cancer Center or Texas Children's Cancer Center under institutional review board–approved protocols) were thawed quickly and placed in fresh RPMI 1640 plus 10% fetal bovine serum, 1% L-glutamine, and 1% pen strep. After recovery for 2 to 3 hours, viable cells were counted and plated in triplicate (5000 viable cells/plate) in methylcellulose media (H4034; StemCell Technologies) with 3 μM EPZ00477 or DMSO vehicle control. After 12 to 14 days, plates were scored for colony number and morphology. Cells were isolated from plates; stained for CD45, CD14, CD13; and analyzed by flow cytometry. Cell morphology was examined by hematoxylin and eosin staining of cytospins (Cytopro).

Nude rat xenografts

In vivo studies were conducted after review by the Animal Care and Use Committee at Charles River Discovery Research Services (Durham, NC). OCI-AML3 cells were implanted subcutaneously into the right flank of female athymic nude rats (Hsd:RH-*Foxn1rnu*, Harlan Laboratories, Inc.). EPZ-5676 was delivered by continuous IV infusion via a catheter surgically implanted in the femoral vein of each rat. Animals were separated into either an efficacy or pharmacokinetic/pharmacodynamic cohort. Both cohorts were dosed by continuous IV infusion with 35 or 70 mg/kg per day of EPZ-5676. A control group received continuous IV infusion of the vehicle 5% hydroxypropyl-β-cyclodextrin in saline. Efficacy was determined after 21 days of drug treatment followed by a 7-day drug holiday. Animals assessed for pharmacokinetics/pharmacodynamics were dosed for 14 days and euthanized following the completion of infusion. Rats were weighed and tumors calipered twice weekly. At the completion of the study, animals were euthanized and tumor tissue collected in a ribonuclease-free environment, bisected, snap frozen in liquid nitrogen, pulverized, and stored at −80°C. Effects on H3K79 methylation, enzyme-linked immunosorbent assay, and gene expression by quantitative reverse transcription polymerase chain reaction (qRT-PCR) were performed (supplemental Methods).

Statistics

Student *t* test and 1-way analysis of variance were used for statistical comparisons where appropriate.

Results

Dot1l messenger RNA expression and H3K79 methylation are increased in *Dnmt3a*$^{-/-}$ HSCs

Reanalysis of previously performed RNA-seq of *Dnmt3a*$^{-/-}$ HSCs[27] (Hoechst side population-KSL CD150$^+$ after Mx1-Cre–mediated deletion and serial transplantation) revealed that *Dot1l* was overexpressed in the *Dnmt3a*$^{-/-}$ relative to WT HSCs isolated from mice of various ages (Figure 1A-B). *Dot1l* overexpression was confirmed by qRT-PCR of 2 biologic replicates of purified *Dnmt3a*$^{-/-}$ and WT HSCs (Figure 1C). In addition, modest reduction of DNA methylation and increased H3K79me2 density at the *Dot1l* promoter suggest that

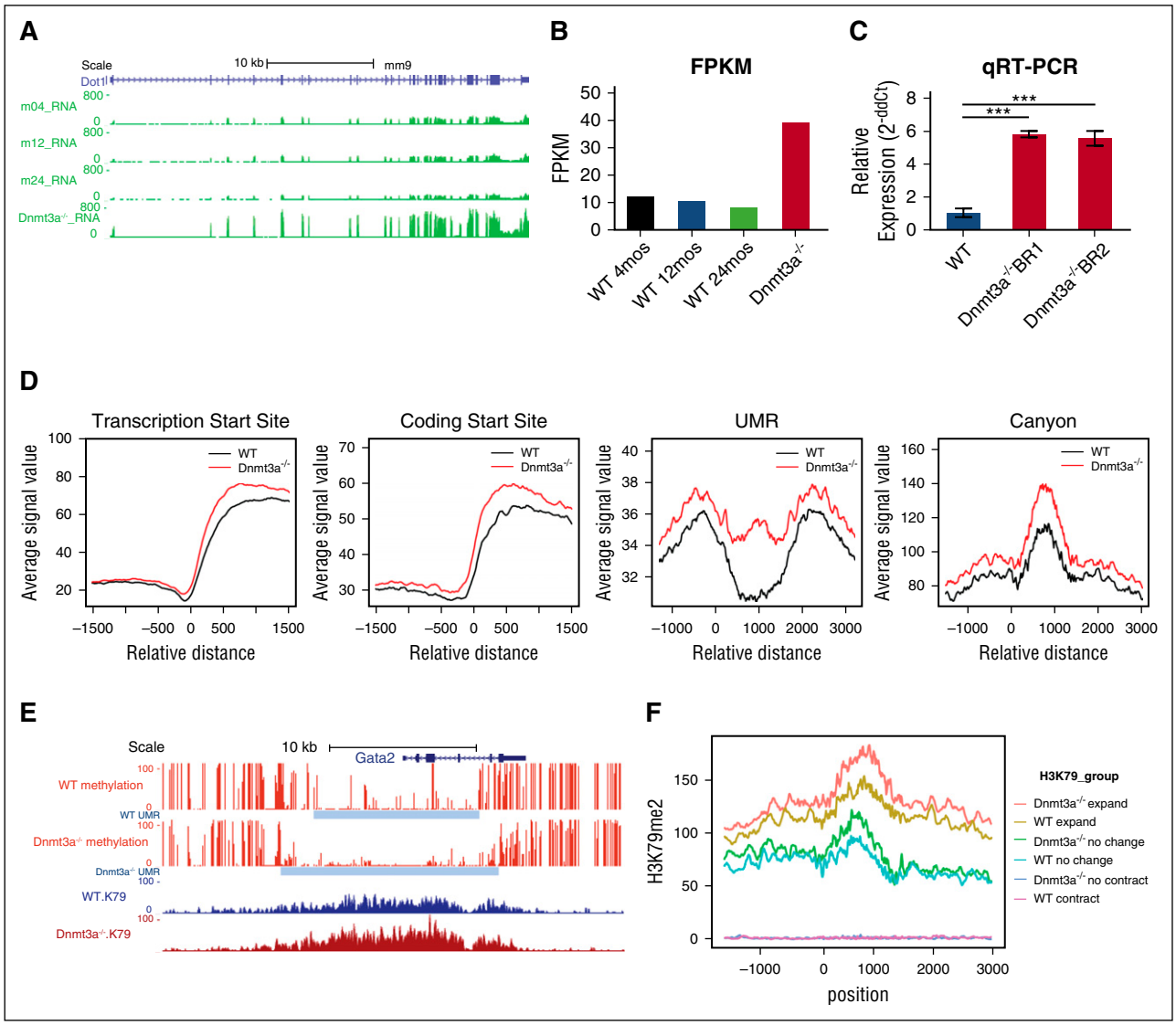

Figure 1. *Dnmt3a*$^{-/-}$ HSCs are characterized by increased Dot1l expression and increased H3K79 methylation. (A) RNA-seq signal density tracks of messenger RNA expression of Dot1l in murine *Dnmt3a*$^{-/-}$ HSCs purified as Hoechst side population-KSL and CD150^{+}. *Dnmt3a*$^{-/-}$ HSCs were purified after Mx-Cre–mediated deletion and serial transplantation as have previously reported[9,27] compared with HSCs from WT HSCs from 4-, 12-, and 24-month-old mice (m04_RNA, m12_RNA, and m24_RNA, respectively). (B) Average FPKM (fragments per kilobase of transcript per million mapped reads) value of Dot1L in WT vs *Dnmt3a*$^{-/-}$ HSCs (2 independently obtained biological replicates of each cohort represented). mos, months. (C) Dot1l expression determined by qRT-PCR relative to glyceraldehyde-3-phosphate dehydrogenase expression in WT HSCs (12 months of age) compared with 2 biologic replicates of *Dnmt3a*$^{-/-}$ HSCs purified after Mx-Cre–mediated deletion and serial transplantation (calculated by $2^{-\Delta\Delta Ct}$ equation). Assay performed in triplicate. Error bars represent standard deviation. (D) ChIP-seq of H3K79me2 of *Dnmt3a*$^{fl/fl}$-Rosa26-Cre-ER^{T2} and *Dnmt3a*$^{wt/wt}$-Rosa26-Cre-ER^{T2} HSCs isolated from primarily transplanted mice after tamoxifen-induced deletion. Average normalized signal density of H3K79me2 at transcription start sites, protein coding start sites, undermethylated regions (UMR) and DNA methylation canyons in *Dnmt3a*$^{-/-}$ HSCs (red) and WT HSCs (black). (D) Representative DNA methylation canyon that expands with *Dnmt3a* deletion (DNA methylation, red; canyon extend, gray) and associated H3K79me2 in WT HSCs (blue) and *Dnmt3a*$^{-/-}$ HSCs (dark red). (E) Average normalized H3K79me2 signal at DNA methylation canyons that expand with *Dnmt3a* deletion (*Dnmt3a*$^{-/-}$ expand, red; WT expand, gold), canyons that do not change with *Dnmt3a* deletion (*Dnmt3a*$^{-/-}$ no change, green; WT no change, teal), and canyons that contract with *Dnmt3a* deletion (*Dnmt3a*$^{-/-}$ contract, blue; WT contract, purple). *P* value was determined using unpaired 2-way Student *t* test. ***$P < .001$.

increased expression of *Dot1l* in this model may be attributable to altered epigenetic regulation (supplemental Figure 1A).

Given the aberrant expression of this histone methyltransferase, we examined whether Dot1L-induced H3K79 methylation was also altered in *Dnmt3a*$^{-/-}$ HSCs compared with WT controls and if these alterations were associated with altered DNA methylation. We previously reported that the edges of large undermethylated regions, termed DNA methylation canyons, are hotspots for DNA methylation loss in *Dnmt3a*$^{-/-}$ HSCs. However, only a portion of these canyons lose methylation and expand with Dnmt3a loss, and a close association between canyon DNA methylation changes and the associated histone marks was identified.[12] Expanding canyons are characterized by the presence of the activating H3K4 tri-methyl (me3) mark and absence of the repressive histone mark H3K27me3,[12] suggesting that Dnmt3a is particularly important in maintaining DNA methylation specifically at canyons with activating histone marks and active gene transcription. We speculated that H3K79me may be another key component of this activating histone signature. To determine if DOT1L-induced H3K79me was altered in *Dnmt3a*$^{-/-}$ HSCs, we performed ChIP-seq for H3K79me2 on *Dnmt3a*$^{fl/fl}$-Rosa26-Cre ER^{T2} and *Dnmt3a*$^{wt/wt}$-Rosa26-Cre ER^{T2} HSCs isolated from transplanted mice after tamoxifen-induced deletion. The H3K79me2 data were aligned with

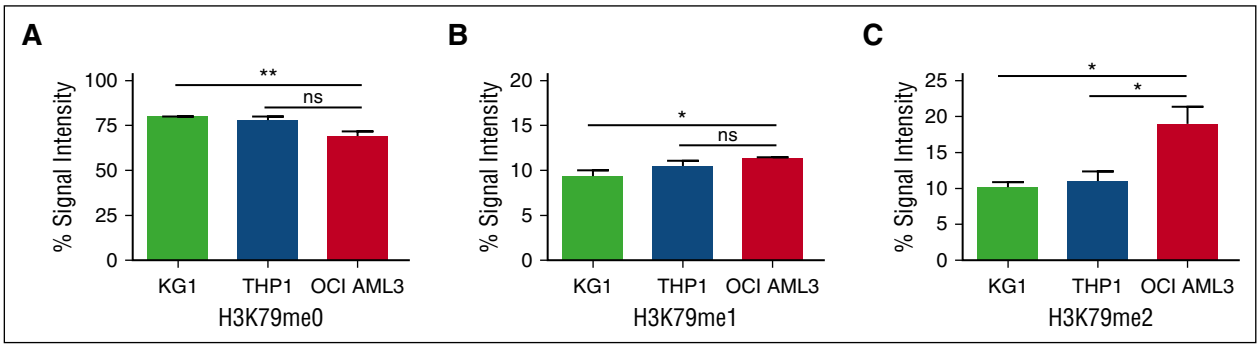

Figure 2. DOT1L-induced H3K79 methylation is increased in *DNMT3A*-mutant human AML. Relative level of (A) unmethylated H3K79, (B) monomethylated H3K79, and (C) dimethylated H3K79 measured by mass spectrometry in 3 AML cell lines (KG1, THP1, and OCI AML3). Data are from a single biological replicate and 3 to 4 technical replicates. Error bars show standard deviation. *P* value was determined using unpaired 2-way Student *t* test. $^{**}P < .01$; $^{*}P < .05$. ns, not statistically significant.

existing whole genome DNA methylation data from *Dnmt3a*$^{-/-}$ HSCs,[12] revealing that levels of H3K79me2 were markedly increased at transcription start sites, protein coding start sites, and at undermethylated regions) (Figure 1D). Importantly, a substantial increase in signal intensity was noted, particularly at DNA methylation canyons (Figure 1D; supplemental Figure 1B-D). We then looked at the association between H3K79me2 and canyon dynamics with *Dnmt3a* loss. We found that H3K79me2 is found at very low levels in canyons that show little change or increased methylation after *Dnmt3a* loss; however, H3K79me2 densely coats canyons that expand when *Dnmt3a* is ablated, such as the canyon associated with the *Gata2* gene (Figure 1E-F). This strong correlation between H3K79me and altered DNA methylation suggests a functional interaction.

DOT1L-induced H3K79 methylation is increased in *DNMT3A*-mutant AML

Based on our murine findings, we postulated that DOT1L might play a role in human *DNMT3A*-mutant AML. To explore this hypothesis, we examined the relative methylation of H3K79 of the *DNMT3A*-mutant human cell line OCI AML3, which harbors the most common and well-characterized type of *DNMT3A* mutation, the dominant-negative acting R882 mutation[5,6] compared with the *MLL*r cell line, THP1, and KG-1 cells that have WT *DNMT3A* and *MLL*. Mass spectrometry demonstrated that OCI AML3 *DNMT3A*-mutant cells had decreased unmethylated H3K79 and increased H3K79me2 in the compared with *DNMT3A* WT cells (Figure 2A-C; supplemental Figure 2). These results are consistent with the increased H3K79me density observed in our murine *Dnmt3a*$^{-/-}$ model, despite the fact that DOT1L expression at the messenger RNA level was not increased in this cell line relative to *DNMT3A* WT AML cell lines (not shown).

Pharmacologic DOT1L inhibition reduces cellular H3K79me and decreases the proliferation of *DNMT3A*-mutant AML cells in a dose- and time-dependent fashion

To explore H3K79 methylation as a potential therapeutic target in *DNMT3A*-mutant AML, we tested the efficacy of pharmacologic DOT1L inhibition in vitro using 2 specific DOT1L inhibitors with comparable potency and specificity: SYC-522[21] and EPZ004777.[23] We treated the only known human cell lines with *DNMT3A* mutations, R882 mutant OCI AML3, and OCI AML2 cells which have a functionally uncharacterized non-R882 mutation (and a possible cryptic *MLL* rearrangement[28]), with SYC-522 or EPZ004777. DOT1L inhibitor treatment resulted in a dose- and time-dependent reduction in H3K79me2 in both cell lines (supplemental Figure 3; Figure 3A, respectively).

Both compounds inhibited growth in a dose-dependent fashion, with more pronounced effects in the OCI AML3 cells compared with the OCI AML2 cells (supplemental Figures 4 and 5). To fully analyze the time-dependent impact of DOT1L inhibitor treatment on *DNMT3A*-mutant AML cells, we performed proliferation assays for 14 days, treating the *DNMT3A*-mutant cell lines with 3 μM EPZ004777 or vehicle control. We also included the DOT1L inhibitor-sensitive *MLL*r cell line, MV411, as a positive control, and the *MLL*- and *DNMT3A*-WT cell line, HL60, as a negative control. There was no impact on the growth of the HL60 cells and modest slowing of growth of the OCI AML2 cells, whereas the proliferation of the OCI AML3 cells was profoundly inhibited from around 7 days of treatment, comparable to effects in the MV411 cell line (Figure 3B). These results indicate that inhibition of DOT1L effectively suppresses the growth of *DNMT3A*-mutant cells.

Treatment with pharmacologic inhibitors of DOT1L induces apoptosis, cell-cycle arrest, and terminal differentiation of *DNMT3A*-mutant AML cell lines

We next sought to determine the specific mechanism of DOT1L inhibitor–induced cytotoxicity in *DNMT3A*-mutant AML cells. By annexin-V binding (AVB) flow cytometry assay, DOT1L inhibition with either SYC-522 or EPZ004777 led to a dose-dependent induction of apoptosis in both OCI AML2 and OCI AML3 cells, though higher doses were required in the OCI AML2 cells to achieve significant apoptosis (supplemental Figures 5B and 6). Treatment with 3 μM EPZ004777 led to substantial induction of apoptosis in the OCI AML3 cells in a time-dependent fashion beginning around 5 days of treatment, earlier than observed in the MV411 cell line (Figure 4A). The HL60 cells had no induction of apoptosis, and the OCI AML2 cells experienced minimal induction of apoptosis (Figure 4A). We also examined the impact of DOT1L inhibitor treatment on cell-cycle kinetics by flow cytometry for DNA content. Both OCI AML2 and OCI AML3 cells experienced cell-cycle arrest with increased percentages of cells in sub-G1 and decreased percentages in S and G2/M phase in a dose- and time-dependent fashion, with the greatest percentage in the OCI AML3 cells (supplemental Figure 6B; Figure 4B, respectively). Additionally, both OCI AML2 and OCI AML3 cell lines showed evidence of induced differentiation with increased expression of the mature monocyte marker CD14, equivalent to the effects of DOT1L inhibition seen in the MV411 cells (Figure 4C).

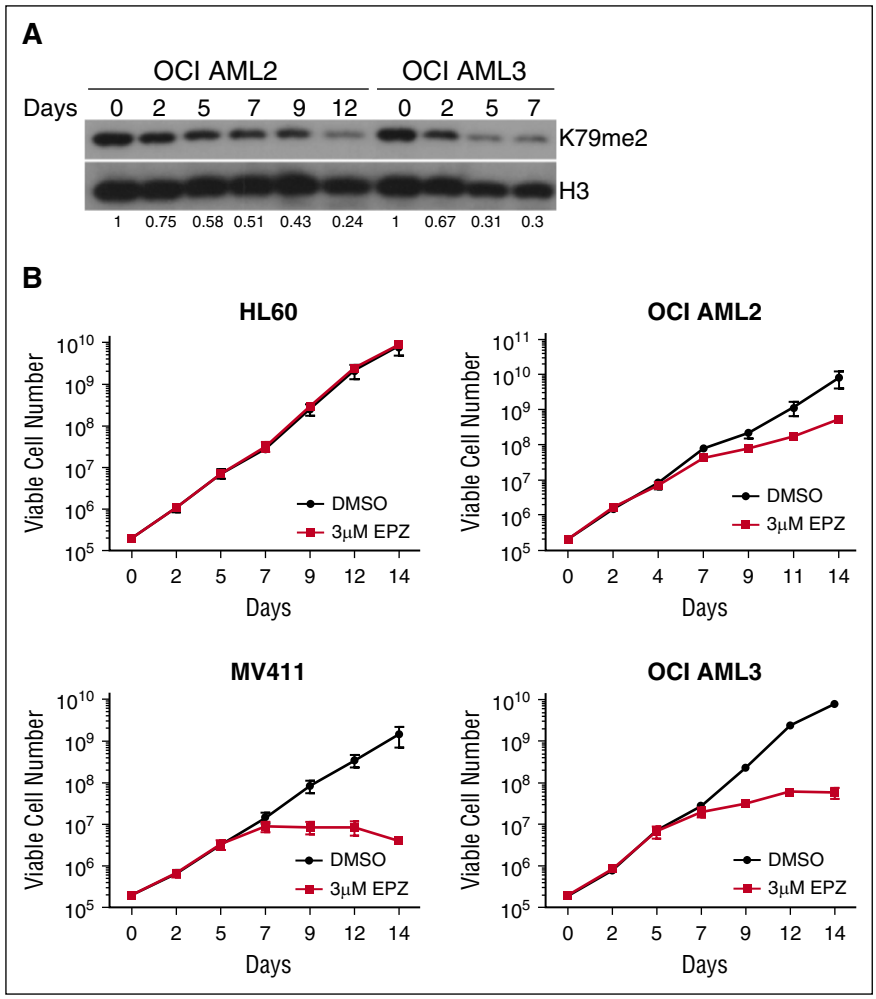

Figure 3. Pharmacologic DOT1L inhibition reduces cellular H3K79me2 and suppresses proliferation of *DNMT3A*-mutant human AML cell lines. (A) Immunoblot analysis of cellular H3K79me2 in OCI AML2 and OCI AML3 cells after treatment with 3 μM EPZ004777. Fraction of H3K79me2/total H3 relative to DMSO-treated control is indicated below each lane. (B) Growth curves of HL60, MV411, OCI AML2, and OCI AML3 cells treated with 3 μM EPZ004777 or vehicle control for 14 days. Numbers are plotted on logarithmic scale. Assays were done in triplicate. Error bars represent standard deviation.

Gene expression analysis after pharmacologic DOT1L inhibition

To assess the effects of DOT1L inhibition on gene expression, RNA-seq was performed on OCI AML2 and OCI AML3 cells after treatment with EPZ004777. We specifically probed canyon-associated genes and found that almost all differentially expressed genes had a significantly reduced expression with treatment (Figure 5A). Although a small subset of canyon-associated genes increased in expression, these canyons characteristically lacked H3K79me2 in our murine model. To validate the RNA-seq results, qRT-PCR was performed for specific *HOX* genes and *MEIS1*, confirming that expression of *MEIS1* and *HOX* cluster genes was suppressed in both the OCI AML2 and OCI AML3 cells after treatment (Figure 5B). *HOX B* cluster genes were preferentially suppressed in the OCI AML3 cells, consistent with the data from patient cohorts showing specific overexpression of *HOX B* cluster genes in *DNMT3A*-mutant leukemia[4,8] (Figure 5B). Additionally, Ingenuity Pathway Analysis of differentially expressed genes showed enrichment of genes involved in cell death, cell-cycle arrest and differentiation (Figure 5C), consistent with the phenotypic consequences of DOT1L inhibitor treatment reported previously. Gene Set Enrichment Analysis (GSEA) of genes upregulated after EPZ treatment demonstrated significant enrichment for genes associated with G1-S transition, including upregulation of cyclin-dependent kinase inhibitor CDKN1A. Strong positive enrichment was further observed for genes involved in myeloid differentiation, including increased expression of lysozyme and myeloperoxidase (Figure 5D-E). There was also significant overlap between upregulated genes in both cell lines after EPZ treatment and genes upregulated by knock-down of HOXA9 in the *MLL*r AML cell line MOLM14.[29] Given the known correlation between suppression of HOXA9 expression and therapeutic effect of DOT1L inhibition in *MLL*r cells, this overlap highlights the likely important role of programs downstream of HOXA9 in both *MLL*r leukemia and *DNMT3A*-mutant leukemia (Figure 5E). This is confounded by a possible MLL fusion in the OCI AML2 cells; however, the overlap between this data set and the gene expression changes in the OCI AML3 cells point toward mechanistic overlap between *MLL*r leukemia and AML harboring R882 *DNMT3A* mutations.

DOT1L inhibition suppresses tumor growth in a nude rat AML xenograft

To test the in vivo efficacy of DOT1L inhibition on human *DNMT3A*-mutant AML, we used a nude rat xenograft model in which OCI AML3 cells were injected subcutaneously, forming a leukemic tumor. After tumor engraftment, the rats (n = 8 per treatment cohort) were treated with continuous IV infusion of vehicle control or EPZ-5676, a DOT1L inhibitor currently being tested in phase 1 clinical trials that is structurally similar to EPZ004777 but with improved pharmacokinetic properties and increased potency.[22] Rats were treated at doses of either 35 mg/kg per day or 70 mg/kg per day via continuous IV infusion for 21 days followed by a 7-day drug holiday. Both doses of EPZ-5676 led to

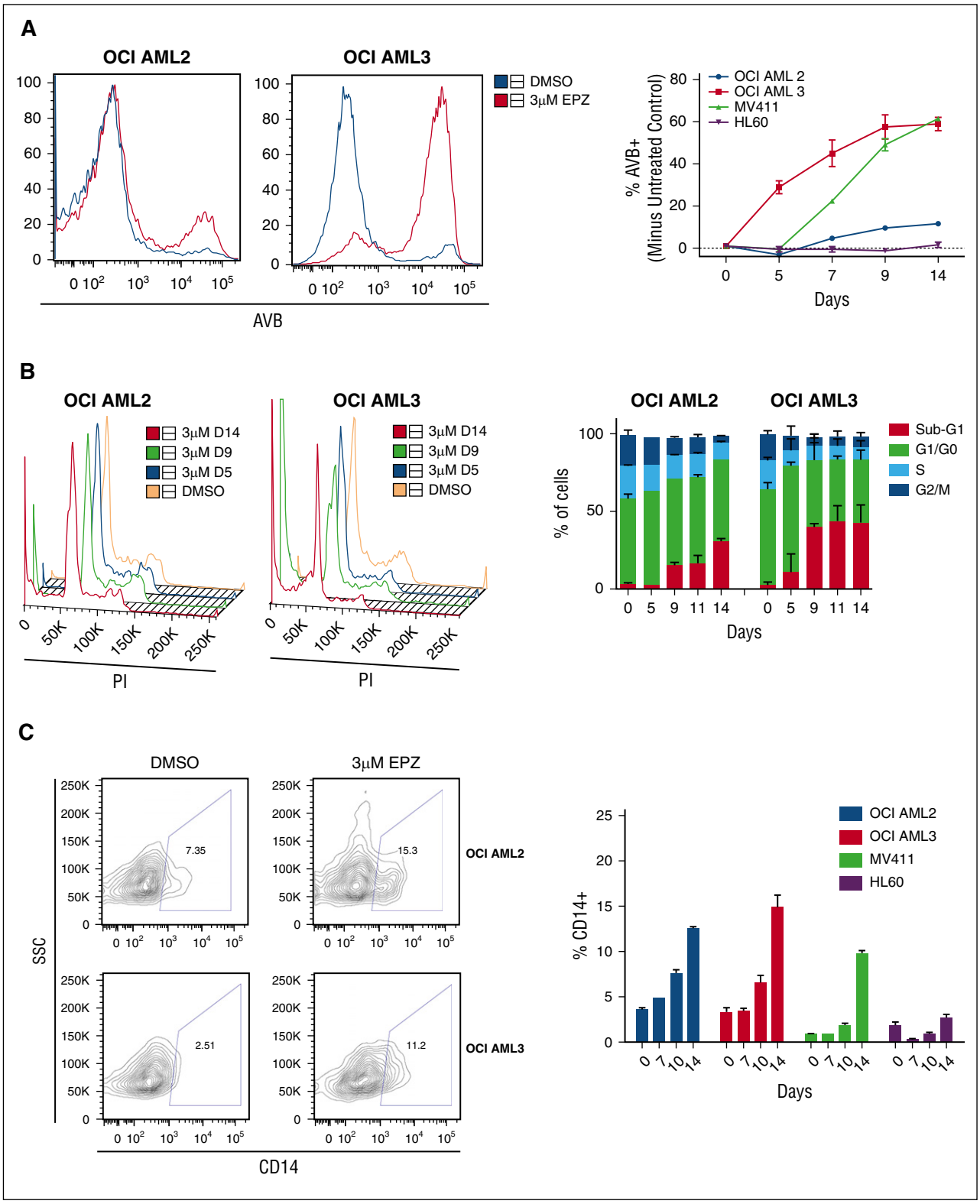

Figure 4. EPZ004777 treatment induces apoptosis, cell-cycle arrest, and terminal differentiation in *DNMT3A*-mutant human AML cells. HL60, MV411, OCI AML2, and OCI AML3 cells were treated with 3 μM EPZ004777 or DMSO vehicle control for 14 days. Cells were replated at a constant concentration in fresh drug-containing media every 2 to 3 days. (A) Representative flow cytometry histograms of AVB for OCI AML2 and OCI AML3 cells on day 14 of treatment with DMSO vehicle control (blue) or EPZ004777 (red) (left). Quantification of % of EPZ004777-treated cells that are AVB^+ minus % AVB^+ vehicle control–treated cells (right). (B) Representative flow cytometry plots of propidium iodide (PI) DNA content cell-cycle analysis for OCI AML2 cells and OCI AML3 cells (left) with quantification of experiments (right) (C) Representative flow plots of CD14 cell surface expression of OCI AML 2 and OCI AML 3 cells treated with DMSO vehicle control or EPZ004777 for 14 days after gating out PI^+ dead cells (left) and quantification of percentage of $CD14^+$ cells treated with 3 μM EPZ004777 or vehicle control at specified time points (right). All assays were done in triplicate. Error bars represent standard deviation. SSC, side scatter.

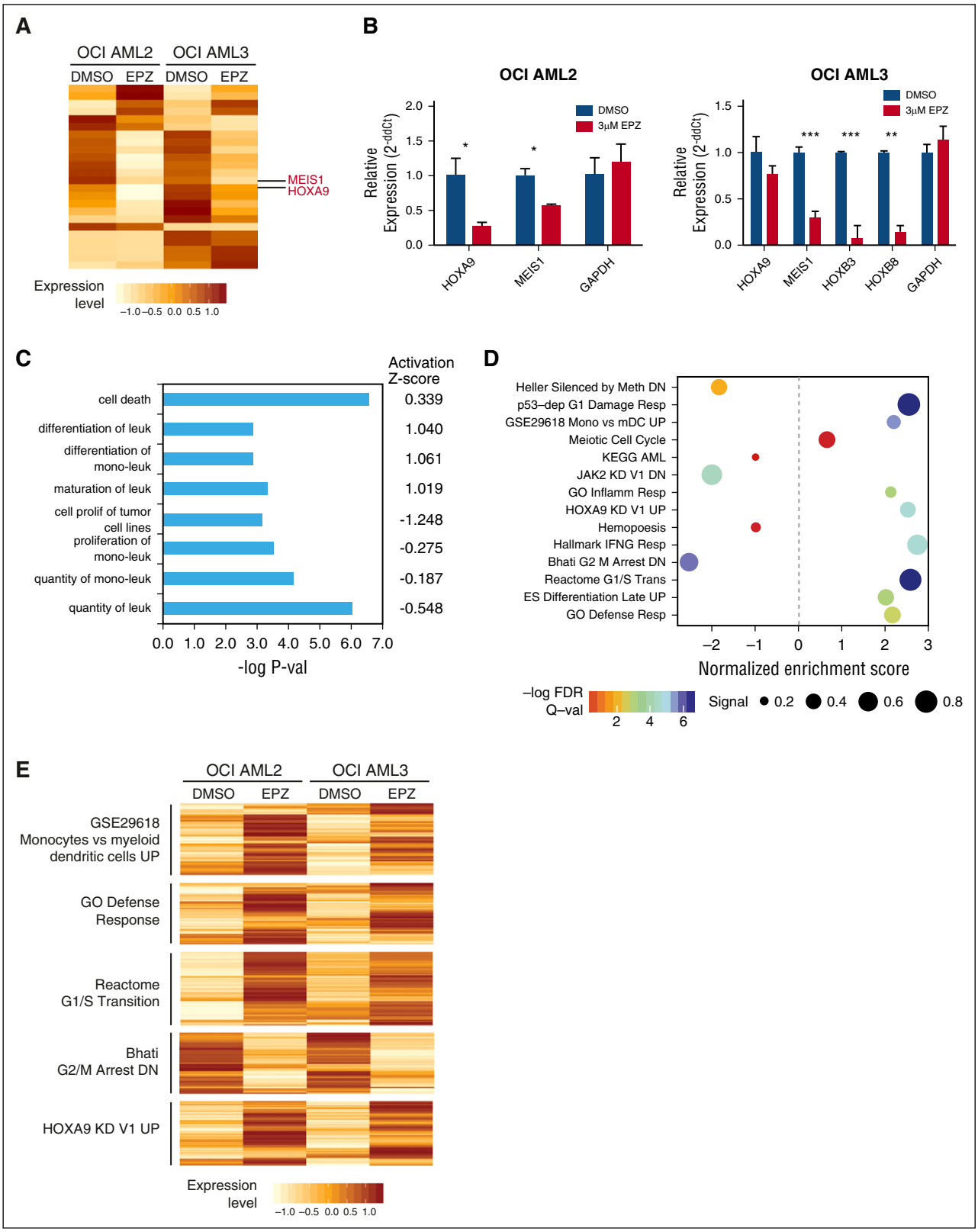

Figure 5. Gene expression changes following DOT1L inhibitor treatment of *DNMT3A*-mutant AML cell lines. (A) Gene expression heat map (gene scaled and centered log2 counts per million) of top differentially expressed canyon-associated genes in OCI AML2 and OCI AML3 cell lines after 14 days of treatment with DOT1L inhibitor. (B) Relative expression determined by qRT-PCR of canyon-associated leukemogenic genes HOXA9, MEIS1, HOXB3, HOXB8, and the housekeeping gene glyceraldehyde-3-phosphate dehydrogenase (GAPDH) in OCI AML 2 and OCI AML3 cells treated with 3 μM EPZ004777 or vehicle control for 14 days. qRT-PCR done in triplicate. Error bars represent standard deviation. (C) Ingenuity Pathway Analysis functional enrichment analysis of genes differentially expressed (false discovery rate [FDR] q value < 0.1) in AML cells after treatment with EPZ004777. P val, *P* value; prolif, proliferation. (D) GSEA of AML cells treated with EPZ004777. (E) Gene expression heat maps (gene scaled and centered log2 counts per million) of representative, core-enriched gene sets from GSEA. DN, downregulated; GO, gene ontogeny; inflamm, inflammatory; leuk, leukocyte; mDC, myeloid dendritic cell; meth, DNA methylation; Q-val, Q value; resp, response; signal size, enrichment signal strength of the leading edge subset of a gene set; trans, transition; UP, upregulated.

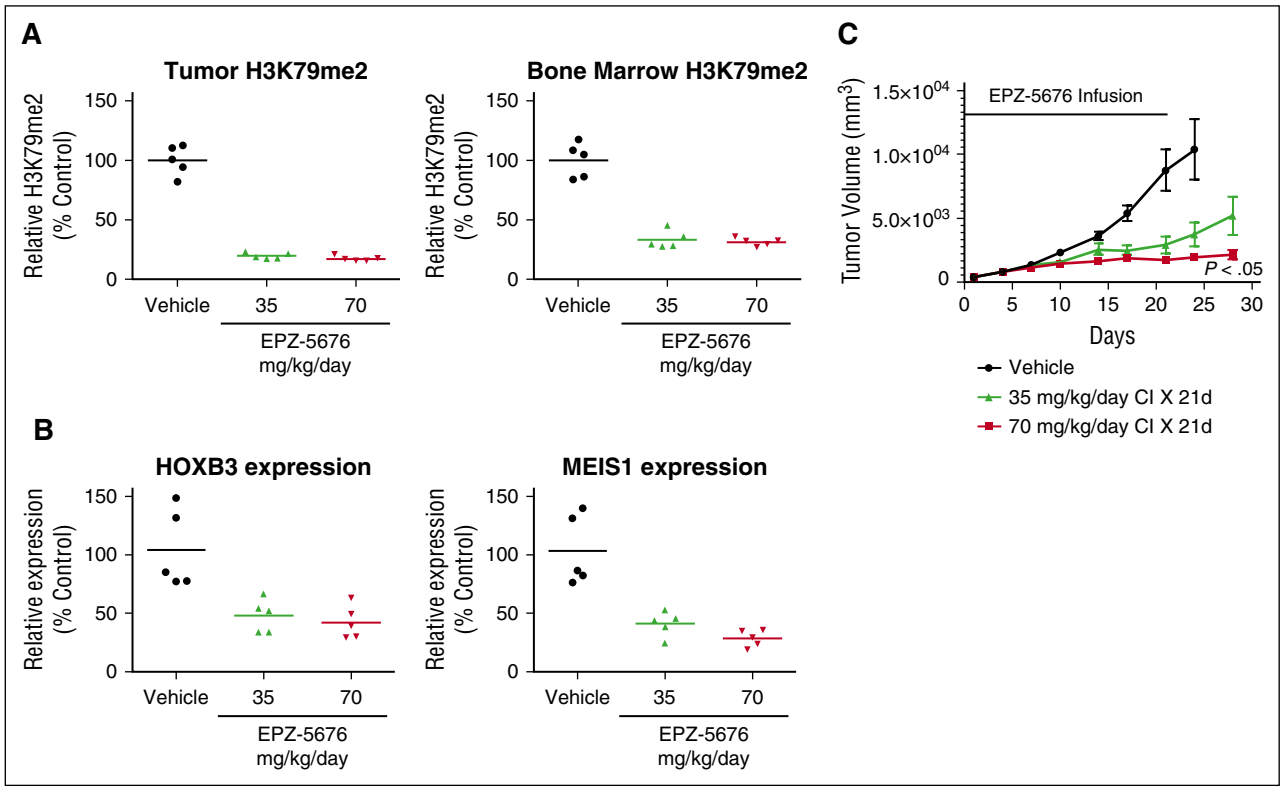

Figure 6. In vivo efficacy of pharmacologic DOT1L inhibition in a rat xenograft model of *DNMT3A*-mutant AML. (A) H3K79me2 levels in acid-extracted histones as measured by enzyme-linked immunosorbent assay in OCI AML3 subcutaneous tumors and bone marrow from vehicle control–treated animals or animals treated with 35 or 70 mg/kg per day EPZ-5676 administered via continuous IV infusion. H3K79me2 levels were normalized to those of total histone H3 in the same sample and are plotted as a percent of the mean H3K79me2 level in tissue from the vehicle-treated group, which is set at 100%. Horizontal lines represent the mean percent H3K79me2 values for each group (N = 5 animals per cohort). (B) Relative expression of MEIS1 and HOXB3 in OCI AML3 subcutaneous tumors in vehicle control–treated mice and mice treated with 35 or 70 mg/kg per day EPZ-5676 for 21 days plotted as a percent of the mean transcript level in tumors from the vehicle-treated group, which is set at 100%. Horizontal lines represent the mean percent transcript level in each group (N = 5 animals per cohort). (C) Volume of OCI AML3 subcutaneous tumors over time in vehicle control–treated animals and animals treated with 35 or 70 mg/kg per day EPZ-5676 administered via continuous IV infusion for 21 days (N = 8 animals per cohort). Error bars represent standard deviation. CI, continuous infusion.

significant reduction of H3K79me2 (Figure 6A) and decreased *MEIS1* and *HOXB3* expression, consistent with in vitro results (Figure 6B). Tumor growth was inhibited in a dose-dependent fashion reaching statistical significance in the 70 mg/kg per day cohort (Figure 6C). These results indicate that DOT1L inhibition is effective at suppressing tumor growth in an in vivo nude rate xenograft model of *DNMT3A*-mutant AML. Ideally, treatment of patient-derived xenograft models would be performed to confirm these results; however, given the need for administration of the drug by continuous infusion for prolonged periods, such studies are currently not feasible.

DOT1L inhibitor treatment selectively reduces the CFC and induces differentiation of primary patient samples with *DNMT3A* mutations

Although our therapeutic experiments using human AML cell lines allowed us to explore the efficacy of DOT1L inhibition in *DNMT3A*-mutant leukemia, given the potential confounding variables inherent to cell lines, we sought to test our hypothesis using primary patient samples. Viably frozen human primary samples were plated in methylcellulose media plus 3 μM EPZ00477 or DMSO vehicle control (patient sample characteristics provided in supplemental Table 2). Samples with *MLL* aberrations and most samples with *DNMT3A* mutations had reduced CFC, whereas normal human cord blood $CD34^+$ cells and primary AML patient samples lacking *MLL* aberration and *DNMT3A* mutation had no change with treatment (Figure 7A). Given potential functional differences of R882 vs non-R882 mutations, we examined *DNMT3A*-mutant samples by mutation type. The average CFC of R882-mutant samples was significantly reduced compared with AML samples WT for both *DNMT3A* and *MLL* and normal $CD34^+$ cord blood cells, similar to the average reduced CFC of MLL-aberrant samples (Figure 7B). Only 2 samples with non-R882 *DNMT3A* mutation were analyzed; therefore, no definitive conclusions about the responsiveness of this genotype can be reached.

Treatment with EPZ004777 also induced differentiation of *DNMT3A*-mutant samples evidenced by increased expression of the mature monocyte marker CD14 compared with vehicle-treated controls, including 1 sample that did not have a significant reduction in CFC (Pt 743509) (Figure 7C; supplemental Figure 7A). Histologic evaluation of the isolated cells also showed evidence of differentiation with a reduced nuclear to cytoplasmic ratio, increased granules in the cytoplasm, and condensation of the nuclei (supplemental Figure 7B). These results indicate that pharmacologic DOT1L inhibition reduces cellular proliferation and promotes differentiation of primary AML patient samples with *DNMT3A* mutations.

Discussion

DOT1L plays a critical role in leukemia with certain *MLL* rearrangements[17-20,30] and is being explored as a therapeutic target

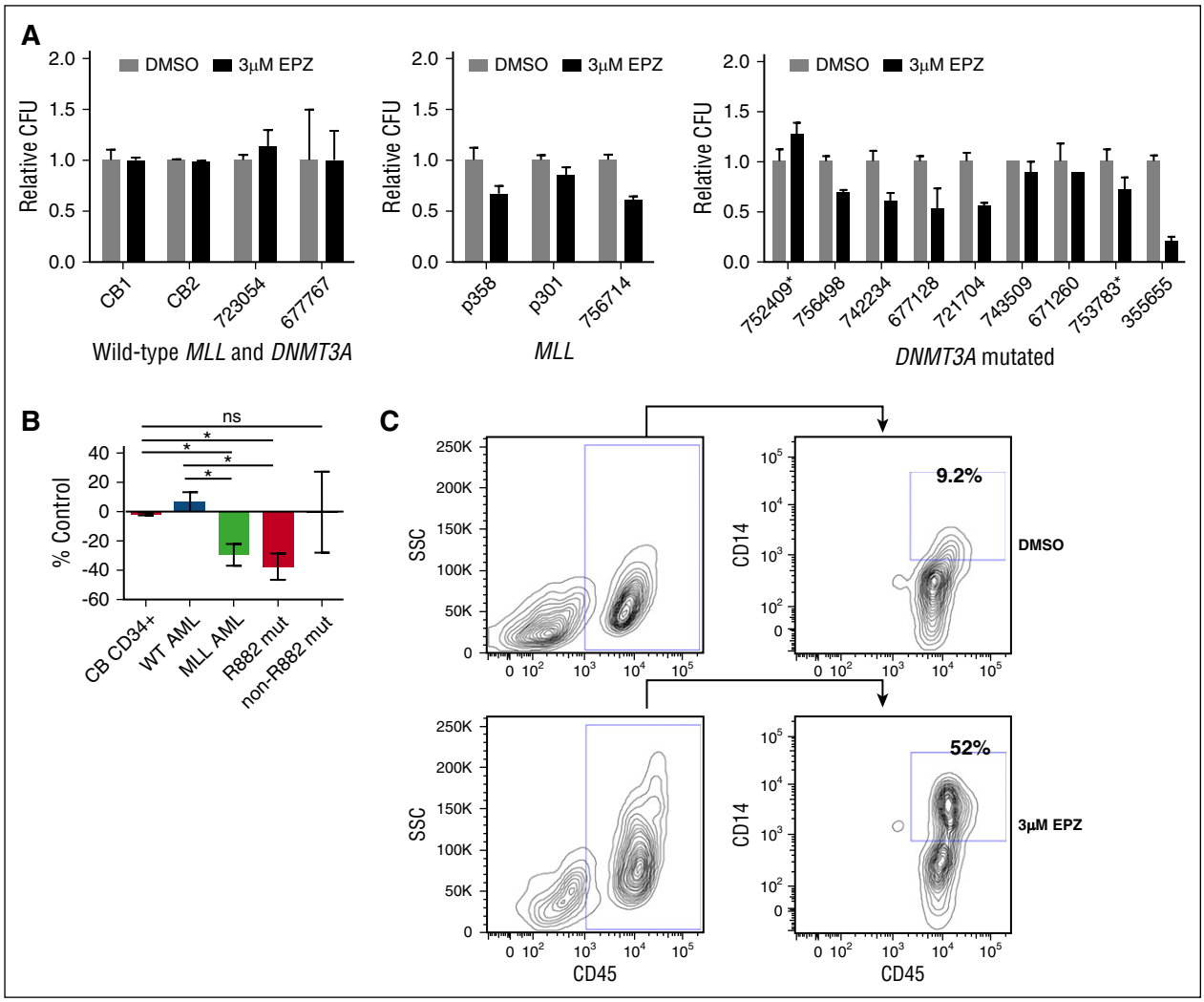

Figure 7. DOT1L inhibitor treatment selectively inhibits in vitro growth and induces terminal differentiation of primary patient samples with *DNMT3A* mutations. (A) Relative colony-forming units (CFU) of normal cord blood CD34$^+$ cells and primary AML samples wild-type for both *DNMT3A* and *MLL* (left), primary AML samples with *MLL* anomalies (middle), and primary AML samples with *DNMT3A* mutations (right). *Non-R882 *DNMT3A* mutation treated with DMSO vehicle control or 3 μM EPZ004777. Assays performed in triplicate; error bars represent standard error of the mean. (B) Average change in CFC of primary patient samples treated with 3 μM EPZ004777 compared with DMSO vehicle–treated control. Error bars represent standard error of the mean. (C) Flow cytometry analysis of CD14 expression of primary AML cells with *DNMT3A* mutation isolated from plates after treatment with DMSO vehicle control or 3 μM EPZ004777. *P* value was determined using unpaired 2-way Student *t* test. *$P < .05$. ns, not statistically significant.

for patients with these genetic alterations.[21-25] Here, we report a possible role for DOT1L in leukemias with mutations of *DNMT3A*. Given the high prevalence of *DNMT3A* mutations across a variety of hematologic malignancies and that in most clinical studies *DNMT3A* mutations are associated with a particularly poor prognosis,[1,3,4,31-33] identifying a novel therapeutic target is of substantial clinical impact. Our data suggest that DOT1L may be an immediately actionable target in *DNMT3A*-mutated AML.

In many *MLL*r leukemias, DOT1L is believed to contribute to leukemogenesis via the fusion partners, including AF9, AF10, and ENL, which normally interact with DOT1L.[17,18,20] The fusions lead to aberrant recruitment of DOT1L and the H3K79me mark to the promoters of MLL target genes such as *MEIS1* and *HOX* cluster genes, ultimately leading to their constitutive expression. However, recent evidence indicates that DOT1L and its cofactor AF10 may play a critical role in regulating *HOX* gene expression via H3K79me2 in a subset of additional leukemias without such MLL fusions, including AMLs with partial tandem duplication of MLL, NUP98-NSD1 fusions, and IDH mutations.[18,30,34,35] We have identified *DNMT3A*-mutant AML as an additional distinct subset of leukemia in which DOT1L may contribute to leukemogenesis via MLL fusion-independent mechanisms.

Using our murine *Dnmt3a*$^{-/-}$ model, we identified a potential functional interaction between H3K79me2 and altered DNA methylation that may explain the site specification in *DNMT3A*-mutant AML. In murine HSCs, H3K79me2 is highly enriched in DNA methylation canyons, and is most prominent in canyons that expand with *Dnmt3a* loss. Expanding canyons coated by H3K79me2 are highly enriched for genes aberrantly expressed in hematologic malignancies, including *HOX* cluster gens.[12] We previously reported that these sites are also characterized by the activating histone mark H3K4 me3 and lack of the repressive H3K27 me3 mark.[12] We expect H3K79me2 is 1 component of an activating histone signature that dictates where in the genome DNMT3A is most critical for maintaining DNA methylation. When DNMT3A function is lost by deletion in a murine model or mutation in human AML, DNA methylation at these sites is eroded. We have further shown that in the *Dnmt3a*$^{-/-}$ HSC hypomethylated canyons

gain additional H3K79 methylation. These observed perturbations of both DNA methylation and covalent histone modifications including H3K79 methylation may contribute to the aberrant expression of the associated genes, including HOX cluster genes. Indeed, when we treated *DNMT3A*-mutant AML cell lines with DOT1L inhibitor, we observed a reduction in the expression of genes associated with expanding H3K79me2-coated canyons including *HOX* and *MEIS1* genes, potentially indicating a direct inhibitory effect. Supportive of this possibility is the finding that, in the R882-mutant cell line, the expression of HOX B cluster genes is affected to a greater extent than HOX A cluster genes, contrary to what is seen in *MLL*r leukemia cell lines. This is consistent with a more extensive loss of DNA methylation in the Hox B cluster–associated DNA methylation canyon compared with the canyon associated with the Hox A cluster in our murine *Dnmt3a*$^{-/-}$ HSCs[12] and more pronounced overexpression of HOX B cluster genes in *DNMT3A*-mutant AML compared with HOX A cluster genes.[4] However, as recent work has demonstrated, HOX gene expression in AML might simply reflect the HOX expression pattern of the HSC/progenitor cell from which the AML arose[36]; therefore, it is possible that the decreased expression of HOX genes observed in response to DOT1L inhibitor therapy reflects differentiation of the cells rather than a direct cause of DOT1L inhibition on gene expression. Furthermore, although in our murine model, *Dot1l* was overexpressed in *Dnmt3a*$^{-/-}$ HSCs relative to WT, we did not observe overexpression of *DOT1L* in human *DNMT3A*-mutant AML cell lines relative to *DNMT3A* WT cell lines nor in *DNMT3A*-mutant patient samples relative to WT in The Cancer Genome Atlas RNA-seq data. Thus, it is possible that *DNMT3A*-mutant AML may exploit DOT1L by alternative mechanisms such as aberrant recruitment. It is also possible that the therapeutic responses observed in *DNMT3A*-mutant cell lines and primary patient samples after treatment with DOT1L inhibitor could be attributable to other yet-unidentified factors. Additional work to fully define the mechanistic role of DOT1L in *DNMT3A*-mutant leukemia is ongoing.

We hypothesized that DOT1L-induced H3K79me might be a therapeutic target in human *DNMT3A*-mediated hematologic malignancies. Our results support this hypothesis, with pharmacologic DOT1L inhibitors leading to inhibition of cellular proliferation, induction of apoptosis, cell-cycle arrest, and terminal differentiation in *DNMT3A*-mutant cell lines and primary patient samples. In particular, the effects observed in the R882 *DNMT3A*-mutant cell line and patient samples were comparable to DOT1L inhibitor-sensitive *MLL*-rearranged cell lines and patient samples. We observed much less effect in the non-R882 mutant OCI AML2 cells, potentially suggesting there may be differences in response based on biological differences between types of *DNMT3A* mutations. However, our ability to evaluate the effect of DOT1L inhibitor therapy on non-R882 mutant AML is limited by a lack of available cell lines without additional confounding mutations and a paucity of patient samples with any given non-R882 *DNMT3A* mutation because no other true mutational hotspots exist.

Although our data indicate that sensitivity of the cell lines to DOT1L inhibition can be conferred by mutant *DNMT3A*, we cannot exclude contributions from other genetic or epigenetic aberrations. Whereas 1 study suggested that OCI AML2 cells harbor a *MLL*r,[28] they lack cytogenetic evidence of 11q23 anomaly and exhibited only modest antiproliferative response to EPZ treatment. The OCI AML3 cell line, in addition to the *DNMT3A* mutation, also harbors a nucleophosmin (*NPM1*) mutation. Both *DNMT3A* and *NPM1* mutations have been associated with overexpression of *HOX* cluster genes and altered DNA methylation[4,6,8,37-39]; however, as 2 of the most commonly cooccurring mutations in human AML,[7] it is difficult to ascertain if these biologic features are attributable to the *DNMT3A* mutation or the *NPM1* mutation—or are secondary to the combined effect of these likely cooperative events. Therefore, although the cell line experiments provided important evidence that *DNMT3A*-mutant AML might be sensitive to DOT1L inhibition, validation in human primary AML samples was essential. Using several *DNMT3A*-mutant samples specifically lacking other known confounding mutations, we observed near-universal reductions in CFC and induction of differentiation in the *DNMT3A* mutant primary AML patient samples consistent with the antiproliferative and pro-differentiation effects observed in our cell lines experiments. Furthermore, our initial data indicating a link between aberrant DNA methylation and H3K79 methylation come from our *Dnmt3a*$^{-/-}$ murine model, which only differ from the WT control by lack of *Dnmt3a*. Together, these observations suggest that the majority of therapeutic effect noted with DOT1L inhibitor therapy is attributable to the biology of the *DNMT3A* mutation.

In summary, based on novel observations from our *Dnmt3a*$^{-/-}$ murine model, we hypothesized that DOT1L may play a role in *DNMT3A*-mutant human leukemia and therefore may represent a therapeutic target. Our in vitro and in vivo work with both cell lines and primary patient samples support this hypothesis and provide the preclinical rationale for possible clinical investigation of pharmacologic DOT1L inhibitors for *DNMT3A*-muant leukemia. Ongoing adult and pediatric phase 1 clinical trials of the DOT1L inhibitor, EPZ-5676, for patients with *MLL*-rearranged hematologic malignancies could greatly facilitate the translation of these findings into clinical investigations for patients with *DNMT3A* mutations in the near term. Ultimately, if our results are validated, DOT1L inhibitors could be incorporated into the multiagent therapeutic regimen for the treatment of this relatively refractory group of patients.

Acknowledgments

The authors thank members of the Goodell Laboratory for helpful discussions; Y. Zheng, A. Guzman, and R. Gupta for technical support; C. Gillespie for critical review of the manuscript; M. Redell and M. Minden for providing cell lines; and J. Matthews and S. Piece for assistance with patient samples.

This work was supported by The Faust Foundation (R.E.R.); Edward P. Evans Foundation, Samuel Waxman Cancer Research Foundation, Henry Malvin Helis Foundation, and Lester and Sue Smith Foundation (M.A.G.); and the National Institutes of Health (NIH), National Cancer Institute (grants CA090433-11 [R.E.R.] and CA183252, CA183252, and CA126752), National Institute of Diabetes and Digestive and Kidney Diseases (grants DK092883 and DK084259), National Human Genome Research Institute (grants R01HG007538 and HG007538); and the Cytometry and Cell Sorting Core at Baylor College of Medicine with funding from the NIH, National Institute of Allergy and Infectious Diseases (grant nos. P30 AI036211 and P30 CA125123), National Institute of General Medical Sciences (S10 RR024574), and the expert assistance of J. Sederstrom and A. White.

Authorship

Contribution: R.E.R. designed and performed experiments, analyzed results, made figures, and wrote the paper; B.A.R. analyzed the data and made figures; M.L., M.J., A.R., J.H.R., C.T.C., S.R.D., S.S., and T.C. designed and performed experiments; L.D. and Y.S. synthesized and provided DOT1L inhibitor compounds; M.A. and S.M.K.

provided patient samples; W.L. helped analyze the data; and M.A.G. designed the experiments and wrote the paper. All authors commented on the edited manuscript.

Conflict-of-interest disclosure: C.T.C. and S.R.D. are employees of Epizyme, Inc. The remaining authors declare no competing financial interests.

Correspondence: Margaret A. Goodell, Department of Pediatrics and Stem Cells and Regenerative Medicine Center, Baylor College of Medicine, One Baylor Plaza, N1030, Houston, TX 77030; e-mail: goodell@bcm.edu; and Rachel E. Rau, Department of Pediatrics, Baylor College of Medicine, 1102 Bates St, Suite 1025, Houston, TX 77030; e-mail: rerau@bcm.edu.

References

1. Ley TJ, Ding L, Walter MJ, et al. DNMT3A mutations in acute myeloid leukemia. *N Engl J Med.* 2010;363(25):2424-2433.
2. Patel JP, Gönen M, Figueroa ME, et al. Prognostic relevance of integrated genetic profiling in acute myeloid leukemia. *N Engl J Med.* 2012;366(12):1079-1089.
3. Ribeiro AF, Pratcorona M, Erpelinck-Verschueren C, et al. Mutant DNMT3A: a marker of poor prognosis in acute myeloid leukemia. *Blood.* 2012; 119(24):5824-5831.
4. Yan XJ, Xu J, Gu ZH, et al. Exome sequencing identifies somatic mutations of DNA methyltransferase gene DNMT3A in acute monocytic leukemia. *Nat Genet.* 2011;43(4): 309-315.
5. Kim SJ, Zhao H, Hardikar S, Singh AK, Goodell MA, Chen T. A DNMT3A mutation common in AML exhibits dominant-negative effects in murine ES cells. *Blood.* 2013;122(25):4086-4089.
6. Russler-Germain DA, Spencer DH, Young MA, et al. The R882H DNMT3A mutation associated with AML dominantly inhibits wild-type DNMT3A by blocking its ability to form active tetramers. *Cancer Cell.* 2014;25(4):442-454.
7. Cancer Genome Atlas Research Network. Genomic and epigenomic landscapes of adult de novo acute myeloid leukemia. *N Engl J Med.* 2013;368(22):2059-2074.
8. Qu Y, Lennartsson A, Gaidzik VI, et al. Differential methylation in CN-AML preferentially targets non-CGI regions and is dictated by DNMT3A mutational status and associated with predominant hypomethylation of HOX genes. *Epigenetics.* 2014;9(8):1108-1119.
9. Challen GA, Sun D, Jeong M, et al. Dnmt3a is essential for hematopoietic stem cell differentiation. *Nat Genet.* 2011;44(1):23-31.
10. Celik H, Mallaney C, Kothari A, et al. Enforced differentiation of Dnmt3a-null bone marrow leads to failure with c-Kit mutations driving leukemic transformation. *Blood.* 2015;125(4):619-628.
11. Mayle A, Yang L, Rodriguez B, et al. Dnmt3a loss predisposes murine hematopoietic stem cells to malignant transformation. *Blood.* 2015;125(4): 629-638.
12. Jeong M, Sun D, Luo M, et al. Large conserved domains of low DNA methylation maintained by Dnmt3a. *Nat Genet.* 2014;46(1):17-23.
13. Chang Y, Sun L, Kokura K, et al. MPP8 mediates the interactions between DNA methyltransferase Dnmt3a and H3K9 methyltransferase GLP/G9a. *Nat Commun.* 2011;2:533.
14. Chen T. Mechanistic and functional links between histone methylation and DNA methylation. *Prog Mol Biol Transl Sci.* 2011;101:335-348.
15. Guo X, Wang L, Li J, et al. Structural insight into autoinhibition and histone H3-induced activation of DNMT3A. *Nature.* 2015;517(7536):640-644.
16. Noh KM, Wang H, Kim HR, et al. Engineering of a histone-recognition domain in Dnmt3a alters the epigenetic landscape and phenotypic features of mouse ESCs. *Mol Cell.* 2015;59(1):89-103.
17. Bernt KM, Zhu N, Sinha AU, et al. MLL-rearranged leukemia is dependent on aberrant H3K79 methylation by DOT1L. *Cancer Cell.* 2011; 20(1):66-78.
18. Deshpande AJ, Chen L, Fazio M, et al. Leukemic transformation by the MLL-AF6 fusion oncogene requires the H3K79 methyltransferase Dot1l. *Blood.* 2013;121(13):2533-2541.
19. Okada Y, Feng Q, Lin Y, et al. hDOT1L links histone methylation to leukemogenesis. *Cell.* 2005;121(2):167-178.
20. Okada Y, Jiang Q, Lemieux M, Jeannotte L, Su L, Zhang Y. Leukaemic transformation by CALM-AF10 involves upregulation of Hoxa5 by hDOT1L. *Nat Cell Biol.* 2006;8(9):1017-1024.
21. Anglin JL, Deng L, Yao Y, et al. Synthesis and structure-activity relationship investigation of adenosine-containing inhibitors of histone methyltransferase DOT1L. *J Med Chem.* 2012; 55(18):8066-8074.
22. Daigle SR, Olhava EJ, Therkelsen CA, et al. Potent inhibition of DOT1L as treatment of MLL-fusion leukemia. *Blood.* 2013;122(6):1017-1025.
23. Daigle SR, Olhava EJ, Therkelsen CA, et al. Selective killing of mixed lineage leukemia cells by a potent small-molecule DOT1L inhibitor. *Cancer Cell.* 2011;20(1):53-65.
24. Yao Y, Chen P, Diao J, et al. Selective inhibitors of histone methyltransferase DOT1L: design, synthesis, and crystallographic studies. *J Am Chem Soc.* 2011;133(42):16746-16749.
25. Liu W, Deng L, Song Y, Redell M. DOT1L inhibition sensitizes MLL-rearranged AML to chemotherapy. *PLoS One.* 2014;9(5):e98270.
26. Ventura A, Kirsch DG, McLaughlin ME, et al. Restoration of p53 function leads to tumour regression in vivo. *Nature.* 2007;445(7128): 661-665.
27. Sun D, Luo M, Jeong M, et al. Epigenomic profiling of young and aged HSCs reveals concerted changes during aging that reinforce self-renewal. *Cell Stem Cell.* 2014;14(5):673-688.
28. Andersson A, Edén P, Lindgren D, et al. Gene expression profiling of leukemic cell lines reveals conserved molecular signatures among subtypes with specific genetic aberrations. *Leukemia.* 2005; 19(6):1042-1050.
29. Faber J, Krivtsov AV, Stubbs MC, et al. HOXA9 is required for survival in human MLL-rearranged acute leukemias. *Blood.* 2009;113(11): 2375-2385.
30. Deshpande AJ, Deshpande A, Sinha AU, et al. AF10 regulates progressive H3K79 methylation and HOX gene expression in diverse AML subtypes. *Cancer Cell.* 2014;26(6):896-908.
31. Walter MJ, Ding L, Shen D, et al. Recurrent DNMT3A mutations in patients with myelodysplastic syndromes. *Leukemia.* 2011; 25(7):1153-1158.
32. Grossmann V, Haferlach C, Weissmann S, et al. The molecular profile of adult T-cell acute lymphoblastic leukemia: mutations in RUNX1 and DNMT3A are associated with poor prognosis in T-ALL. *Genes Chromosomes Cancer.* 2013; 52(4):410-422.
33. Haferlach T, Nagata Y, Grossmann V, et al. Landscape of genetic lesions in 944 patients with myelodysplastic syndromes. *Leukemia.* 2014; 28(2):241-247.
34. Chang MJ, Wu H, Achille NJ, et al. Histone H3 lysine 79 methyltransferase Dot1 is required for immortalization by MLL oncogenes. *Cancer Res.* 2010;70(24):10234-10242.
35. Sarkaria SM, Christopher MJ, Klco JM, Ley TJ. Primary acute myeloid leukemia cells with IDH1 or IDH2 mutations respond to a DOT1L inhibitor in vitro. *Leukemia.* 2014;28(12):2403-2406.
36. Spencer DH, Young MA, Lamprecht TL, et al. Epigenomic analysis of the HOX gene loci reveals mechanisms that may control canonical expression patterns in AML and normal hematopoietic cells. *Leukemia.* 2015;29(6): 1279-1289.
37. Falini B, Mecucci C, Tiacci E, et al; GIMEMA Acute Leukemia Working Party. Cytoplasmic nucleophosmin in acute myelogenous leukemia with a normal karyotype. *N Engl J Med.* 2005; 352(3):254-266.
38. Alcalay M, Tiacci E, Bergomas R, et al. Acute myeloid leukemia bearing cytoplasmic nucleophosmin (NPMc+ AML) shows a distinct gene expression profile characterized by up-regulation of genes involved in stem-cell maintenance. *Blood.* 2005;106(3):899-902.
39. Figueroa ME, Lugthart S, Li Y, et al. DNA methylation signatures identify biologically distinct subtypes in acute myeloid leukemia. *Cancer Cell.* 2010;17(1):13-27.